Available online at www.sciencedirect.com
ScienceDirect
Journal of the European Ceramic Society 29 (2009) 2069–2077
www.elsevier.com/locate/jeurceramsoc

Effect of milling energy on mechanical activation of ($Mo + Si_3N_4$) powders during the synthesis of Si_3N_4–$MoSi_2$ *in situ* composites

Sheela Singh [a,*], M.M. Godkhindi [a], R.V. Krishnarao [b], B.S. Murty [c]

[a] *Department of Metallurgical and Materials Engineering, Indian Institute of Technology, Kharagpur 721302, India*
[b] *Defence Metallurgical Research Laboratory, Kanchanbagh, Hyderabad 500058, India*
[c] *Department of Metallurgical and Materials Engineering, Indian Institute of Technology, Madras, Chennai 600036, India*

Received 29 May 2008; received in revised form 2 November 2008; accepted 5 November 2008
Available online 13 December 2008

Abstract

Attempts have been made to study the effect of milling energy and type of grinding media on the mechanical activation during the production of $MoSi_2$ from a reaction between Mo and Si_3N_4. Powder mixtures of Mo and Si_3N_4 in the molar ratios of 1:1, 1:2 and 1:3 were ball milled using WC, steel, and ZrO_2 grinding media for mechanical activation. In order to evaluate the results obtained after high-energy ball milling and pyrolysis of these milled powder mixture, milling parameters have been converted to two energy parameters, namely, impact energy of the ball and total energy of milling. The optimum impact energy of ball required for mechanical activation of $Mo + xSi_3N_4$ ($x = 3, 2, 1$) powder mixtures by WC grinding media was found to be in the range of 0.145–0.173 J, which leads to a reduction of pyrolysis temperature by 100–200 °C. Samples milled with higher impact energy than the optimum range led to formation of undesirable phases, which dilutes the effect of mechanical activation. Samples milled with both steel and ZrO_2 grinding media having lower impact energies than the optimum show the presence of enormous contamination during milling and phases like $ZrSi_2$, Fe_3Si and Fe_5Si_3 were observed after pyrolysis without any significant reduction in pyrolysis temperature required for $MoSi_2$ synthesis.

Keywords: Composites; Structural application; Silicides; Si_3N_4; Milling

1. Introduction

The properties, which have made $MoSi_2$ a well-known structural material, are low density (6.31 g cm^{-3}), high melting point (2030 °C) and excellent oxidation resistance at elevated temperatures.[1–3] It can be produced *in situ* in several ways such as combustion synthesis,[4] spark plasma sintering,[5] mechanical alloying[6–9] and mechanical activated synthesis.[10–12] Mechanical alloying is the most widely used technology to produce nanostructures, amorphous and non-equilibrium metastable phases.[8,9] There are several attempts on the production of $MoSi_2$ by mechanical alloying including a few on the analysis of energy required for $MoSi_2$ synthesis.[13] It was observed that the energy transferred during milling influence the mechanical alloying process.[13–16]

However, the synthesis by mechanical alloying is limited to the systems, which possess negative free energy of formation at ambient temperature.[17] The recently developed Mechanically Activated Synthesis (MAS),[18] Mechanical Activated Annealing Process (MA2P)[11] and Mechanical Activated Self propagating High temperature Synthesis (MASHS)[19] is suitable for reactions that have a positive free energy of formation at ambient temperature and could generate nanostructured at low energy consumption.

Si_3N_4–$MoSi_2$ composite materials possess potential high temperature applications.[20] Its most widely used method of production includes two-stage hot pressing/hot isostatic pressing of (Si_3N_4 and $MoSi_2$) powder mixture preferably in the temperature range of 1400–1700 °C.[21] The composites produced by *in situ* synthesis offer advantages over conventional powder processing in terms of morphology, agglomeration, SiO_2 content, particle size and process cost. If mechanical activated *in situ* synthesis of $MoSi_2$ from $Mo + Si_3N_4$ powders can be achieved at lower temperature (in comparison to HP/HIP condition) then synthesis and densification of Si_3N_4–$MoSi_2$ composites can be

* Corresponding author. Presently at NFTDC, Kanchanbagh, Hyderabad-58, India.
E-mail address: sheela2k5@gmail.com (S. Singh).

0955-2219/$ – see front matter © 2008 Elsevier Ltd. All rights reserved.
doi:10.1016/j.jeurceramsoc.2008.11.005

accomplished in a single process. The present papers aims to investigate the effect of milling energy and grinding media on the mechanical activated synthesis of $MoSi_2$ using ($Mo + Si_3N_4$) powders in different molar ratio and also to optimize milling parameter required for mechanical activation of $Mo + Si_3N_4$ powder mixture. The present study is newer in a sense that for the first time mechanical activation parameter has been optimized and milling map has been developed for MAS of Si_3N_4–$MoSi_2$ *in situ* composites from $Mo + Si_3N_4$ powder mixtures.

2. Experimental details

Sinterable grade Mo powder (1–3 μm) and Si_3N_4 powder (<1.5 μm) were used in the present study. The energy dispersive spectroscopic analysis of the Mo powder showed 99.9% Mo and 0.1% oxygen. Mixtures of powders of Mo and Si_3N_4 in the molar ratio of 1:1, 1:2, and 1:3 (MoSN1, MoSN2 and MoSN3 respectively) were chosen to produce Si_3N_4–$MoSi_2$ *in situ* composites. Powder mixtures were milled with steel, ZrO_2 and WC grinding media in a Fritsch (P5) planetary ball mill. Milling was carried out in toluene at a speed of 300 rpm with a ball to powder ratio (BPR) of 10:1 and 15:1 for various lengths of time (10–70 h). For high productivity and effective milling the charging volume was limited to 2/3rd of the volume of vial. It has already been reported that overfilling of vial badly influences the milling process and also attributes to balls reciprocal hindering.[13,22] 50 numbers of balls of each type were used for the present study. For a given BPR, the powder quantity was adjusted accordingly. The other details of the milling conditions are mentioned in (Table 1). To evaluate milling energy,[15] the linear velocity of balls was calculated according to the procedure given by Burgio et al.[16] The samples were collected every 10 h of milling, were taken out and analysed by X-ray diffraction (XRD) using a Philips diffractometer (PW 1840) with Co Kα radiation. The milled samples were compacted into pellets of 10 mm diameter at a uniaxial pressure of 598 MPa for 60 s. The relative density of each pellet was approximately 65% T.D. (Theoretical density). The compacts were subjected to pyrolysis under argon atmosphere at different temperatures (1200–1600 °C) at a heating rate of 20 °C/min. The pyrolysed samples were analysed by XRD. The microstructure of the composite was studied by a JEOL JSM 5800 scanning electron microscope (SEM). Energy dispersive X-ray microanalysis (EDS) of samples was carried out to estimate the phase composition.

3. Results

3.1. Effect of milling

3.1.1. X-ray diffraction

Fig. 1(a)–(c) shows the XRD patterns of MoSN1, MoSN2 and MoSN3 samples, respectively, as a function of milling time for BPR of 10:1 with WC grinding media. The intensities of peaks of Mo decreased to a great extent after milling for 10 h whereas the peaks of Si_3N_4 decreased to small extent. A less intense peak of WC appeared after 10 h of milling and its intensity increases with increase in milling duration and Si_3N_4 content. Further milling beyond 10 h caused a decrease in peak intensity of Mo and an increase in peak breadth, suggesting a decrease in its crystallite size. After 30 h of milling Mo peaks more or less disappeared from the XRD pattern for MoSN3 and MoSN2. But some peaks of Mo were still observed in MoSN1 sample at this stage. Further milling beyond 30 h was not carried out because disappearance of Mo phase in the two compositions is chosen as critical milling duration.

Fig. 2(a)–(c) are the XRD patterns of MoSN1, MoSN2 and MoSN3 samples, respectively, as a function of milling time milled with WC media at a BPR of 15:1. Up to 10 h of milling the behaviour of the samples milled with the BPR 15:1 was similar to that of samples milled with the BPR 10:1, except that the intensity of X-ray diffraction peaks of WC was more prominent in case of sample milled with BPR 15:1. On further milling the samples to 30 h the X-ray diffraction peaks of Mo did not disappeared. In this case peaks of Mo vanished from the XRD patterns in case of MoSN2 after 60 h of milling and in case of MoSN3 after 70 h of milling. Peaks of Mo were observed in MoSN1 sample even after 70 h of milling. Interestingly, Mo reduces to fine size and disappears from the X-ray diffraction pattern of the samples milled with WC grinding media and BPR 10:1 and 15:1 in the following sequence MoSN2 → MoSN3 → MoSN1. No reaction products or molybdenum silicides phase were detected for the samples milled with BPR of 10:1 and 15:1.

The effect of steel and zirconia grinding media for the MoSN1 composition at a BPR of 10:1 is shown in Fig. 3(a) and (b) respectively. In Fig. 3(a) after 10 h of milling X-ray diffraction peak of iron was observed. With increase in milling to 30 h iron appeared as the major phase with low intensity peaks of Mo and Si_3N_4. When the sample was milled with zirconia grinding media (Fig. 3(b)) large amount of tetragonal zirconia, ZrO_2 (T), was observed after 10 h of milling and appeared, as the major phase with low intensity X-ray diffraction peaks of Mo and Si_3N_4. With increase in milling to 30 h, the X-ray diffraction peak of Molybdenum and Si_3N_4 completely disappeared. Similar results were obtained for MoSN2 and MoSN3 samples milled with steel and zirconia grinding media. Only the amount of contamination pick up in MoSN2 and MoSN3 samples was relatively higher than that of MoSN1 samples.

3.1.2. Crystallite size and micro-strain

Assuming that transformation from microstructure to nanostructure depends on the transferred mechanical energy.[23] The apparent size of Mo crystallites was evaluated from XRD profile analysis is shown in Table 2. A rapid decrease in the crystallite size and increase in microstrain was observed for molybdenum particles with increase in milling time. MoSN1 samples milled with BPR of 15:1 show larger reduction in crystallite size than the samples milled with BPR 10:1. After 30 h of milling Mo crystallites of 56 nm were observed for MoSN1 sample milled with BPR 15:1. No further reduction in crystallite size was observed for the sample milled beyond 30 h. MoSN2 and MoSN1 samples milled for 10 h with BPR 15:1 show greater reduction in crystallite size than that of sample milled with BPR 10:1. Beyond 10 h the reduction in crystallite size was more for the sample milled with BPR 10:1. This may be due to large amount of WC pick in

Table 1
Milling and energy parameters of ($Mo + xSi_3N_4$) samples milled at 300 rpm with different grinding media.

Composition	Sample identity	BPR	Diameter of ball (mm)	Weight of ball (g)	Milling media	Milling time (h)	v_b (ms^{-1})	E'_b(J)	E_t (30 h) kJ/g
MoSN1	M1	15:1	8.14	5.685	WC	0–70	7.27946	0.149	5.750
	M2	10:1	8.11	5.61	WC	0–30	7.27989	0.147	3.839
	M3	10:1	8.0	2.25	ZrO_2	0–30	7.76240	0.067	4.359
	M4	10:1	8.0	3.323	Steel	0–30	7.72718	0.098	4.320
MoSN2	M5	15:1	9.0	7.668	WC	0–70	7.26728	0.200	5.732
	M6	15:1	8.51	6.569	WC	0–10	7.27421	0.172	5.743
	M7	10:1	8.33	6.084	WC	0–30	7.27676	0.159	3.831
MoSN3	M8	15:1	8.56	6.62	WC	0–70	7.27350	0.173	5.742
	M9	10:1	8.07	5.54	WC	0–30	7.28046	0.145	3.836
	M10	10:1	8.50	2.88	ZrO_2	0–30	7.75355	0.0857	4.352
	M11	10:1	8.03	3.367	Steel	0–30	7.71844	0.0995	4.310

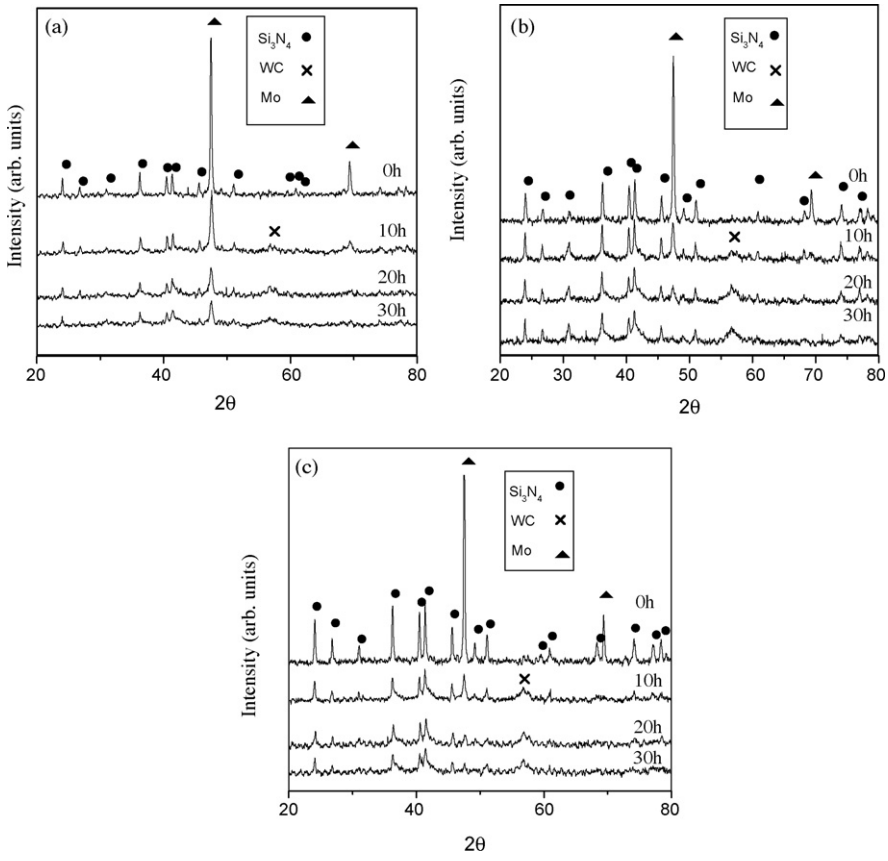

Fig. 1. Plots of XRD patterns obtained after different milling times of (a) MoSN1, (b) MoSN2 and (c) MoSN3 samples milled with WC grinding medium at ball to powder ratio of 10:1.

Table 2
Effect of milling time on crystallite size (dc), % of micro-strain (ε) of molybdenum particles.

Milling hours	MoSN1		MoSN2		MoSN3	
	BPR 15:1 dc (nm), % ε	BPR 10:1 dc (nm), % ε	BPR 15:1 dc (nm), % ε	BPR 10:1 dc (nm), % ε	BPR 15:1 dc (nm), % ε	BPR 10:1 dc (nm), % ε
10	84, 0.300	97, 0.274	96, 0.256	124, 0.326	109, 0.249	151, 0.211
20	74, 0.336	79, 0.312	82, 0.284	73, 0.331	73, 0.324	69, 0.342
30	56, 0.397	66, 0.338	69, 0.339	25, 0.730	66, 0.346	58, 0.386
40	56, 0.397		64, 0.348		62, 0.363	
50	55, 0.399		58, 0.360		54, 0.396	
60	55, 0.399		–		53, 0.403	
70	55, 0.399		–		–	

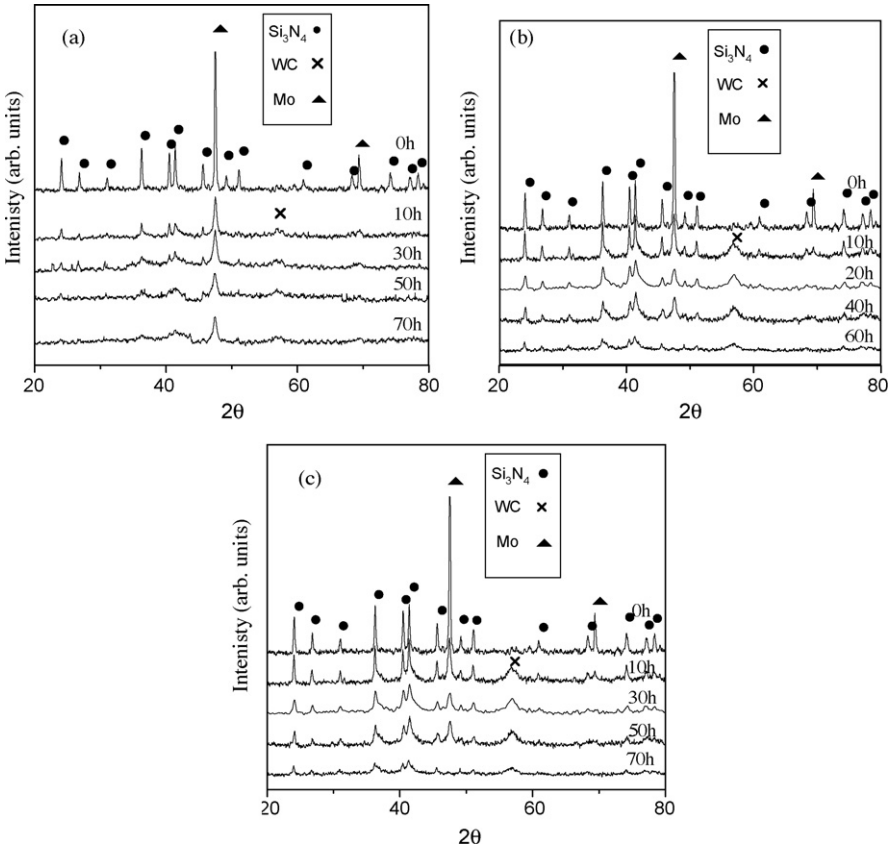

Fig. 2. Plots of XRD patterns obtained after different milling times of (a) MoSN1, (b) MoSN2 and (c) MoSN3 samples milled with WC grinding medium at ball to powder ratio of 15:1.

the MoSN2 and MoSN3 sample milled for 10 h with BPR ratio of 15:1. The contamination pick up in the sample could depend on several factors such as BPR, Impact energy of ball, grinding media and also with nature of reactants.[22]

3.2. Effect of pyrolysis

3.2.1. X-ray diffraction

In our previous work it was observed that irrespective of milling time (10–70 h), all of the milled samples behave in a similar way as a function of temperature.[24] So only results are shown which was obtained after pyrolysis of samples milled for the maximum milling time. The XRD spectra of 70 h milled and pyrolysed (WC grinding media, BPR 15:1) MoSN1 samples as a function of temperature is shown in Fig. 4. In the as-milled samples Mo diffraction peaks were observed. Milled samples after pyrolysis at 1200 °C show the presence of Mo, Si_3N_4 and Mo_5Si_3 phases. Pyrolysis of the samples at 1400 °C led to the formation of minor amounts of $MoSi_2$ along with major Mo_5Si_3 phase. Increase in the temperature to 1500 °C led to the com-

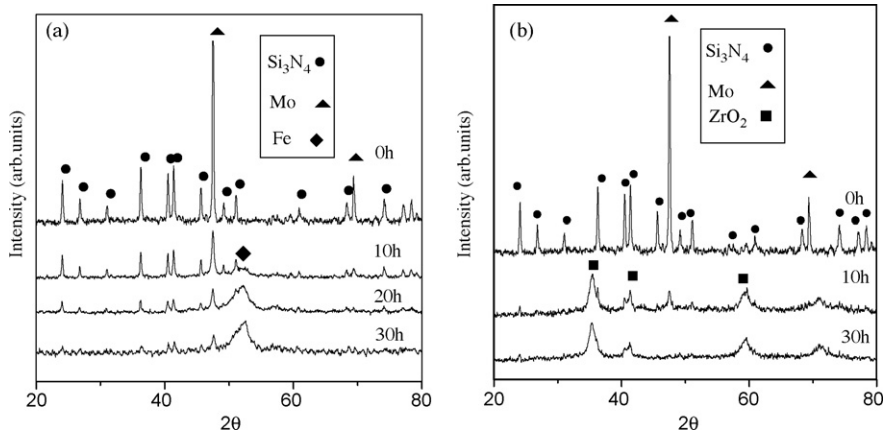

Fig. 3. Plots of XRD patterns obtained after different milling times of MoSN1 samples milled with (a) steel and (b) zirconia grinding media at ball to powder ratio of 10:1.

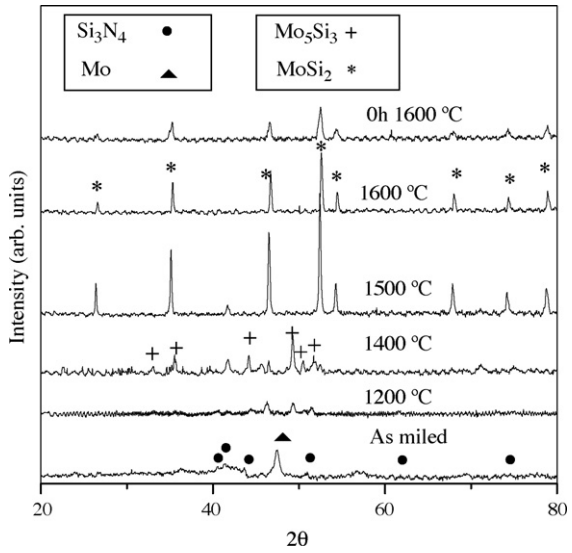

Fig. 4. XRD patterns of MoSN1 samples milled for 70 h with WC grinding media at ball to powder ratio 15:1 after pyrolysis at different temperatures.

plete formation of $MoSi_2$. Further increase in temperature to 1600 °C, caused a decrease in the intensity of $MoSi_2$ phase. In the unmilled MoSN1, complete formation of $MoSi_2$ was observed at 1600 °C. Milling can thus be seen to induce mechanical activation resulting in a decrease in the pyrolysis temperature by 100 °C.

The XRD spectra of 70 h milled and pyrolysed MoSN2 samples (WC balls, BPR 15:1) as functions of temperature are shown in Fig. 5. Peaks of Mo were absent in case of 70 h as-milled MoSN2 samples. Milled samples after pyrolysis at 1200 °C showed the presence of Mo, Si_3N_4 and Mo_5Si_3 phases. With increase in temperature to 1400 °C, Mo_5Si_3 was observed to be the major phase along with the presence of phases of Si_3N_4 and minor amounts of SiC. With further increase in temperature to 1500 °C, tetragonal $MoSi_2$ (T) became the major phase along

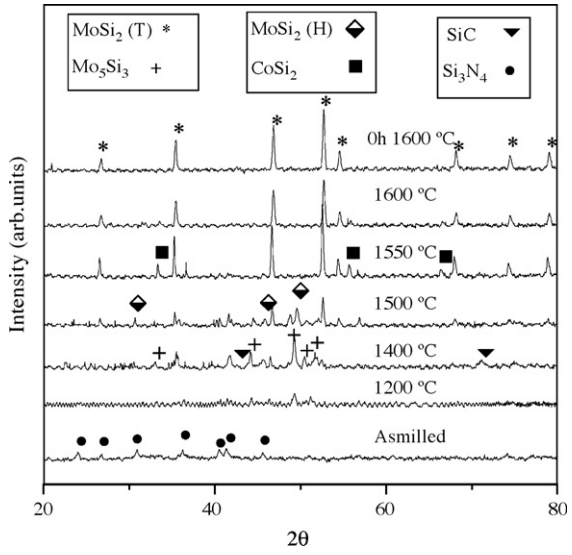

Fig. 5. XRD patterns of MoSN2 samples milled for 70 h with WC grinding media at ball to powder ratio 15:1 after pyrolysis at different temperatures.

with presence of minor phase of $MoSi_2$ (H), Si_3N_4. $MoSi_2$ (H) is not a stable phase at higher temperatures and was absent for the samples pyrolysed at 1550 °C. A new phase corresponding to $CoSi_2$ was observed at 1550 °C. At both 1550 °C and 1600 °C, phases observed were only $MoSi_2$ (T) and $CoSi_2$. Complete conversion to $MoSi_2$ (T) without any phases of lower silicide occurred at 1550 °C. In the unmilled samples complete formation of $MoSi_2$ could be achieved at 1600 °C. Thus the mechanical activation of MoSN2 sample decreased the pyrolysis temperature required to form complete $MoSi_2$ by about 50 °C. Presence of new phase corresponding to $CoSi_2$ and SiC were observed in addition to $MoSi_2$.

The XRD spectra of 70 h milled (WC balls, BPR 15:1) and a pyrolysed MoSN3 sample as a function of temperature is shown in Fig. 6(a). In the as-milled sample peaks of Mo were absent. After pyrolysis at 1200 °C, peaks corresponding to the phases of Mo_2C, Mo_5Si_3 and Si_3N_4 could be observed, although the peaks of Mo_2C were not very distinct. Increase in temperature to 1400 °C led to a complete formation of $MoSi_2$. At 1400 °C phases corresponding to SiC and Si_3N_4 could also be observed. The source of carbon for the formation of SiC could be Mo_2C, which occurs by reduction of WC with Mo (reaction (i)). Mo_2C in turn could react with Si_3N_4 to form $MoSi_2$ and SiC (reaction (ii)). To confirm this possibility, a powder mixture of Mo and WC in the molar ratio of 1:2 was pyrolysed at 1000 °C for 0.5 h and the formation of Mo_2C could be confirmed (Fig. 6(b)). Since Mo has a high solubility for tungsten, peaks of tungsten could not be observed in milled and pyrolysed samples (reaction (iii)).

$$2Mo + WC \rightarrow Mo_2C + W \quad \text{(i)}$$

$$\tfrac{1}{2}Mo_2C + Si_3N_4 \rightarrow MoSi_2 + \tfrac{1}{2}SiC + \tfrac{5}{3}N_2 + \tfrac{1}{6}Si_3N_4 \quad \text{(ii)}$$

$$Mo + W \rightarrow Mo(W) \quad \text{(iii)}$$

Intensities of $MoSi_2$ peaks were found to be maximum for the milled samples pyrolysed at 1400 °C. In the unmilled samples complete formation of $MoSi_2$ was observed at 1600 °C. Thus mechanical activation obtained by WC grinding media caused a decrease in pyrolysis temperature by 200 °C and produces (Si_3N_4–$MoSi_2$/SiC) composite. In addition of molybdenum silicides phases of SiC and intermediate phase of Mo_2C were observed.

Sample milled with steel and zirconia grinding media did not show reduction in pyrolysis temperature required for the $MoSi_2$ formation. Sample milled with steel and zirconia grinding media indicated the formation of prominent Fe_5Si_3 and $ZrSi_2$ phases, respectively, on pyrolysis at 1600 °C (Table 3).

3.2.2. SEM and EDS

Fig. 7(a)–(c) shows the SEM microphotograph of the mechanically activated sample after pyrolysis. It was observed that mechanical activated synthesis has led to the formation of discrete and equiaxed $MoSi_2$ ($\ll 1$ μm) particles (Fig. 7(a)). With increase in milling hours the amount of discrete $MoSi_2$ particle increases (Fig. 7(b)). In Fig. 7(b) ultrafine phase of $MoSi_2$ was observed to present in the matrix of Si_3N_4. The volume fraction of $MoSi_2$ phase was estimated to be more than 50%.

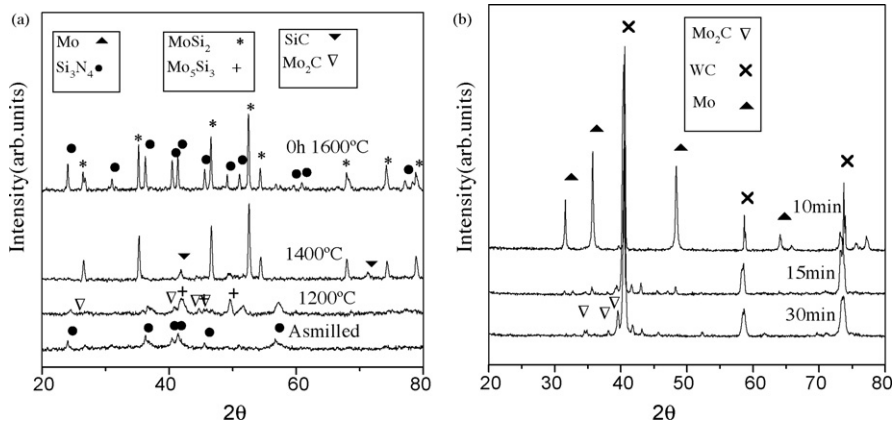

Fig. 6. (a) XRD patterns of MoSN3 samples milled for 70 h with WC grinding media at ball to powder ratio 15:1 after pyrolysis at different temperatures. (b) XRD patterns of (Mo + WC) pyrolysed at 1000 °C for 0–0.5 h.

Table 3
Effect of milling parameters on mechanical activation of ($Mo + Si_3N_4$) powders.

Sample name	E_t kJ/mole of Mo (30 h)	Milling time (h)	Mo peaks			Reduction in pyrolysis temperature (°C)	Product phases obtained upon pyrolysis (vol.%)
			30 h	60 h	70 h		
M1	551.66	10–70	P	P	P	100	$92MoSi_2$, $8\ Si_3N_4$
M2	367.93	10–30	P			100	$>95MoSi_2$, $<5Si_3N_4$
M3	418.20	10–30	NP			0	$75ZrO_2$, 9Zr, $10Si_3N_4$, $6MoSi_2$
M4	414.46	10–30	P			0	$76Fe_5Si_3$, $15Si_3N_4$, $9MoSi_2$
M5	549.93	10–70	P	NP	NP	50	$80MoSi_2$, $6Si_3N_4$, $14CoSi_2$
M6	550.98	10	–	–	–	100	$91MoSi_2$, $9Si_3N_4$
M7	367.55	10–30	NP			100	$>95MoSi_2$, $<5Si_3N_4$
M8	550.88	10–70	P	P	NP	200	$68MoSi_2$, $8Si_3N_4$, 24SiC
M9	417.34	10–30	PLD	–	–	100	$93MoSi_2$, $7Si_3N_4$

P: Present, NP: Not present, PLD: Present but less distinct.

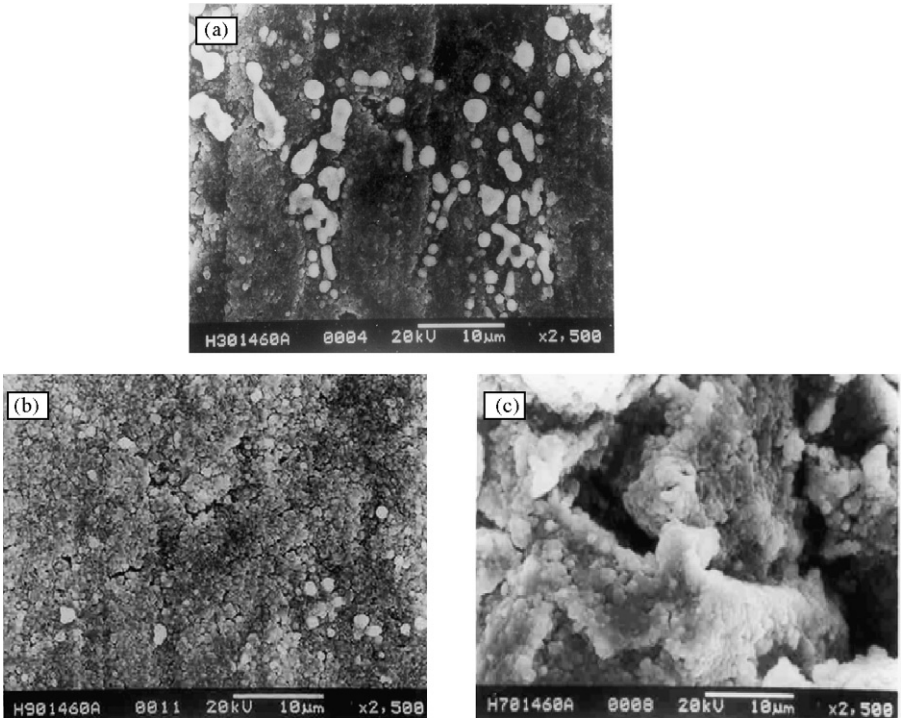

Fig. 7. SEM photomicrographs of milled samples after pyrolysis for 1 h in argon (a) 30 h milled MoSN3 and pyrolysed at 1400 °C, (b) 50 h milled MoSN3 and pyrolysed at 1400 °C and (c) 70 h milled MoSN1 and pyrolysed at 1500 °C.

As per the existing literature if the $MoSi_2$ phase content in more than 26 vol.% then the composite morphology changes from dispersed phase to interconnected network.[1] But in the present study it was observed that upon longer hours of mechanical activation dispersed phase of $MoSi_2$ in Si_3N_4 matrix could be obtained even at higher volume fraction of $MoSi_2$. Similar observation was observed for MoSN2 samples. In MoSN1 sample milled for 70 h and pyrolysed at 1500 °C for 1 h, $MoSi_2$ was present as aggregate of ultrafine and equiaxed particles (Fig. 7(c)). 4.35, 11.36 and 6.12 wt% of tungsten was detected by EDS analysis, respectively, in MoSN1, MoSN2 and MoSN3 sample milled for 70 h (BPR 15:1) after pyrolysis at 1600 °C for 1 h.

4. Discussion

4.1. Energy

All the above results can best be understood if one considers the thermodynamic feasibility of molybdenum silicides formation from $Mo + Si_3N_4$ reactant and the energy transferred during milling. The free energy change of Mo and Si_3N_4 reactions leading to the formation of $MoSi_2$, Mo_5Si_3 and Mo_3Si is sufficiently positive at ambient temperature and becomes slightly negative with increase in temperature.[24] The energy of each ball[15–16] during the milling process is given by

$$E_b = \tfrac{1}{2}(m_b v_b^2) \quad \text{(iv)}$$

where E_b is the energy of each ball, m_b is the mass of one ball and v_b is the linear or absolute velocity of the ball. It (v_b) can be calculated following the process given by Burgio et al.[16] The impact energy of each ball can be given as $E'_b = \Phi_b E_b$, where Φ_b is the correlation factor for different degrees of the filling of the vial.[13–16] The total energy transferred per unit weight of powders for a given time can be expressed as

$$E_t = \frac{\nu E'_b n_b t}{W_p} \quad \text{(v)}$$

where E_t is the total energy transferred per unit weight of powders, n_b the number of balls, t the milling time (h), W_p the weight of powders. The frequency of impact (ν) according to Burgio et al.[16] is given by

$$\nu = \frac{K(\omega_p - \omega_v)}{2\pi} \quad \text{(vi)}$$

K is the proportionality constant and approximately equal to 1, ω_p the angular velocity of the disc and ω_v that of the vial. All the milling parameters are accounted for two energy parameters, i.e. the impact energy of each ball (E'_b) and the total energy transferred (E_t) to the powder after certain duration of milling. These parameters were evaluated and shown in Table 1.

4.2. Milling of Mo containing powder

During the milling process Mo was refined to nano size and disappeared from the X-ray diffraction pattern of samples. Fig. 8 shows the plot of impact energy of ball used during milling vs. total energy transferred per unit weight of ($Mo + xSi_3N_4$) powder mixture. The region in which Mo peaks disappeared after milling the samples with WC grinding media having BPR 10:1 and 15:1 is segregated as region A and B respectively. In region A, it is observed that when the impact energy of WC balls was high, i.e. 0.159 J (M7, MoSN2), the disappearance of Mo peaks occurred after 30 h on imparting a total energy of 3.831 kJ/g to the powder mixture. But when the impact energy of samples was low, i.e. 0.145J (MoSN3, M9) disappearance of Mo peaks was not observed to be completed after 30 h on imparting a total energy of 3.836 kJ/g. It shows that with decrease in impact energy the amount of total energy required to reduce the Mo grain size to the nanometer range (Table 2) increases and therefore it takes longer milling time for the Mo phase to disappear from the X-ray diffraction pattern of the sample (Fig. 1(b) and (c)). When MoSN1 sample was milled with impact energy of 0.147 J/ball (M2), the X-ray diffraction peaks of Mo did not disappear up to 30 h (Fig. 1(a)). It designates that increase in volume fraction of ductile phase in the powder mixture increases rewelding due to which a difference in the intensity of XRD peaks of Mo was observed in 30 h milled MoSN1 (M2, $E'_b = 0.147$ J, $E_t = 3.839$ kJ/g) and MoSN3 (M9, $E'_b = 0.145$ J, $E_t = 3.836$ kJ/g) samples.

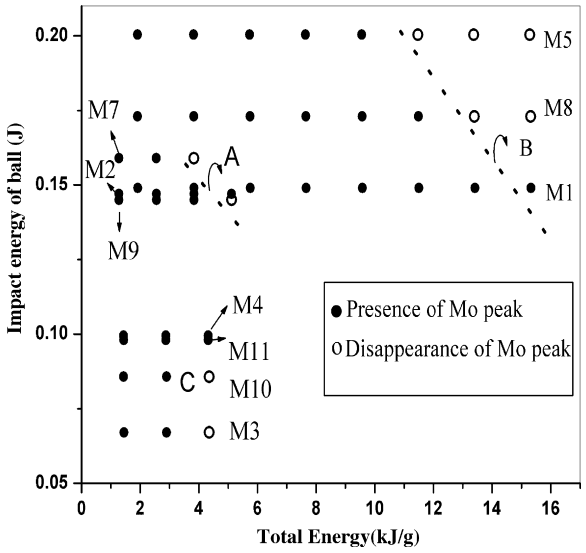

Fig. 8. Impact energy of ball used during milling vs. total energy transferred per unit weight of ($Mo + xSi_3N_4$) powder mixtures.

Similar result was observed for samples milled with BPR 15:1 in Region B (Fig. 8). The impact energies of ball for MoSN3, MoSN2 and MoSN1 samples milled with BPR 15:1 are 0.173, 0.2 and 0.149 J respectively. Mo particles reduced to fine nano size (Table 2) and it peaks disappeared after 70 h (Fig. 2(a)) of milling in MoSN3 (M8, $E_t = 13.401$ kJ/g) and after 60 h (Fig. 2(b)) of milling in MoSN2 (M5, $E_t = 11.232$ kJ/g). Mo peak was observed even after 70 h (Fig. 2(c)) of milling in MoSN1 (M1, $E_t = 13.438$ kJ/g). It indicates that the refinement of Mo to fine nano size and its disappearance from the XRD profile of sample could thus depend on impact energy of ball and total energy supplied during milling.

Interestingly, it was observed that Mo particles require more energy to reduce to nano size and disappear from X-ray diffraction pattern of samples milled with BPR 15:1 (Region B). It was observed that when the impact energy of samples milled with BPR 10:1 (M2) and 15:1 (M1) lies in close proximity to each other (Table 1), samples milled with BPR of 15:1 shows larger reduction in crystallite size than the samples milled with BPR 10:1 (Table 2). This could be due to larger amount of total energy transferred to the sample milled with BPR 15:1 (Table 1) than that of 10:1. But when the values of impact energy of the samples milled with BPR 15:1 (M5 and M8) are much higher than those milled with BPR 10:1 (M7 and M9, Table 1) then samples milled with BPR of 15:1 took longer time to refine Mo to fine nano size (Table 2). This could be due to the reduction in total energy transferred to the powder mixture due to contamination (WC) pick up during milling. The amount of contamination pick up in the sample was largest for the sample milled with highest impact energy of the ball (MoSN2, refer Section 3.2.2). That is why peaks of Mo disappeared much later in the MoSN2 and MoSN3 samples milled with BPR of 15:1 as compared to the samples milled with BPR of 10:1.

The region in which Mo peaks disappeared after milling the samples with steel and zirconia grinding is segregated in region C. In region C, the disappearance of the Mo peak in M3 and M10 sample might not be caused by mechanical activation but by the enormous contamination pick up in the samples during milling (Fig. 3(b)). It further indicates that an abrasive wear of grinding media occurs during milling due to the presence of Si_3N_4. A similar result was observed for samples milled with steel grinding media. The Mo peaks gets diluted due to (Fe) contamination pick up during milling (Fig. 3(a)). So milling with low impact energy of ball (<0.1 J/ball) is not suitable for mechanical activation of $(Mo + xSi_3N_4)$ powder mixture.

Formation of $MoSi_2$ has not been observed during milling even though the total energy (E_t) supplied (Table 3) to the powder mixtures after 30 h of milling is much more than that required for $MoSi_2$ formation at ambient temperature (+300.4 kJ/mole of Mo).[24] It indicates that mechanical activated synthesis of $MoSi_2$ does not only depend on thermodynamics but also on its kinetics parameter.[11]

4.3. Temperature of formation of $MoSi_2$

Milling of powder mixtures with WC media tends to decrease the temperature of formation of $MoSi_2$ by 50–200 °C. Fig. 9 shows impact energy of the samples milled with different grinding media as a function of milling time. The region of mechanical activation, which led to reduction in pyrolysis temperature required for $MoSi_2$ formation without presence of undesirable phases, is shown by dotted contour in the figure. Samples (M1, M2, M6, M7 and M9, Table 3) milled with low impact energy of 0.145–0.16 J/ball have led to the reduction in temperature of 100 °C (Table 3) and product phases are $MoSi_2$ and Si_3N_4. Samples (M8) milled with high impact energy of 0.173 J/ball led to the reduction in pyrolysis temperature of 200 °C, but an additional phase of SiC was observed. Milling the samples (M5) with impact energy of 0.2 J/ball showed a large amount of contamination pick up and only 50 °C decrease in the pyrolysis temperature was noticed. It indicates that for mechanical activation, milling with impact energy of ball in the range of (0.145–0.173 J) appears beneficial both in terms of product quality and pyrolysis temperature. It further designates that milling beyond the optimum impact energy of balls (0.145–0.173 J) dilutes the effect of mechanical activation. With increase in milling time the amount of total energy supplied to the samples increases. But it does not led to further reduction in pyrolysis temperature due to increased contamination. It shows that milling with WC medium for 5–10 h is sufficient to get mechanical activation leading to reduction in pyrolysis temperature.

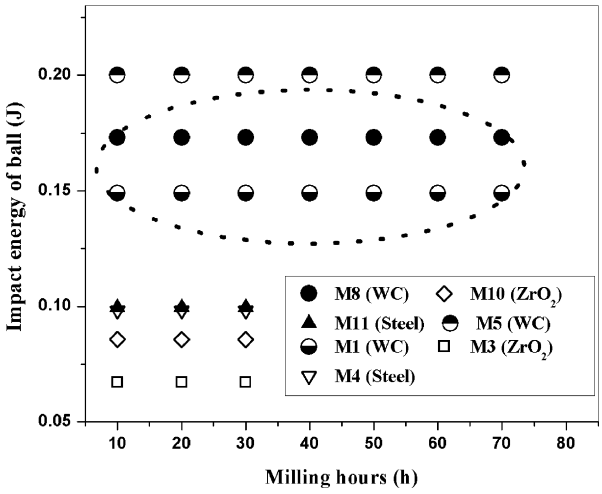

Fig. 9. Impact energy of the $(Mo + Si_3N_4)$ samples milled with different grinding media as a function of milling time.

The impact energy of sample milled with steel and zirconia grinding media is less than 0.1 J/ball. But due to very high contamination of zirconia and iron, mechanical activation has not been effective and impurity phases such as ZrO_2, $ZrSi_2$ and Fe_5Si_3 were observed, respectively, upon pyrolysis (Table 3). These impurity phases were prominent than molybdenum disilicides and silicon nitride phase. No significant reduction in pyrolysis temperature was observed. The reduction in pyrolysis temperature and the final product were not same for all samples and depend on the impact energy of balls during milling.

4.4. Conclusions

Considerable degree of mechanical activation could be achieved in $(Mo + Si_3N_4)$ powders of different compositions ($Mo:Si_3N_4 = 1:1/2/3$) through milling with WC grinding medium. There exists an optimum impact energy range (in the present case 0.145–0.173 J/ball), which leads to reduction in pyrolysis temperature. For the samples milled with impact energy outside the optimum range, the contamination pick up in the samples reduces the effect of mechanical activation. Milling for (10–70) h led to the same reduction in temperature. Further, it has been observed that the impact energy of a ball which only depends on the density of the grinding medium for a given milling conditions, seems to be more important than the total energy transferred in the process of mechanical activation. Steel

and ZrO_2 grinding media having lower impact energy than the optimum do not lead to mechanical activation. For efficient mechanical activation, the wear resistance of the grinding media must be higher than that of the sample chosen for milling. Steel and zirconia grinding media possessing lower wear resistance than Si_3N_4 have led to enormous contamination pick up in the sample during milling.

References

1. Petrovic, J. J., Pena, M. I. and Kung, H. H., Fabrication and microstructure of $MoSi_2$ reinforced Si_3N_4 matrix composites. *J. Am. Ceram. Soc.*, 1997, **80**, 1111.
2. Petrovic, J. J., Honnel, R. E. and Vasudevan, A. K., SiC–reinforced–$MoSi_2$ alloy matrix composites. *Mater. Res. Soc. Symp. Proc.*, 1990, **194**, 123.
3. Krishnarao, R. V. and Subrahmanyam, J., Sintering of $MoSi_2$ by reacting ($Mo + Si_3N_4$) compacts. *MSE*, 2003, **A352**, 340.
4. Jo, S.-W., Lee, G.-W., Moon, J.-T. and Kim, Y.-S., On the formation of $MoSi_2$ by self-propagating high temperature synthesis. *Acta Metall. Mater.*, 1996, **44**, 4317.
5. Kuchino, J., Kurokawa, K., Shibayama, T. and Takahashi, H., Effect of microstructure on oxidation resistance of $MoSi_2$ fabricated by spark plasma sintering. *Vacuum*, 2004, **73**, 623.
6. Yen, B. K., Aizawa, T. and Kihara, J., Synthesis and formation mechanisms of molybdenum silicides by mechanical alloying. *Mater. Sci. Eng.*, 1996, **A220**, 8.
7. Bokhonov, B. B., Konstanchuk, I. G. and Boldyrev, V. V., Sequence of phase formation during mechanical alloying in the Mo–Si system. *J. Alloys Compd.*, 1995, **218**, 190.
8. Ma, E., Pagan, J., Cranford, G. and Atzmon, M., Evidence for self-sustained $MoSi_2$ during high temperature high energy ball milling of elemental powders. *J. Mater. Res.*, 1996, **8**, 1836.
9. Fei, G. T., Liu, L., Ding, X. Z., Zhang, L. D. and Zheng, Q. Q., Preparation of nanocrystalline intermetallic compounds WSi_2 and $MoSi_2$ by mechanical alloying. *J. Alloys Compd.*, 1995, **229**, 280.
10. Gras, Ch., Vrel, D., Gaffet, E. and Bernard, F., Mechanical activation effect on the self sustaining combustion reaction in the Mo–Si system. *J. Alloys Compd.*, 2001, **314**, 240.
11. Gaffet, E. and Malhouroux-Gaffet, N., Nanocrystalline $MoSi_2$ phase formation induced by mechanical activated annealing. *J. Alloys Compd.*, 1994, **205**, 27.
12. Takacs, L., Soika, V. and Balá, P., The effect of mechanical activation on highly exothermic powder mixtures. *Solid State Ionics*, 2001, **141–142**, 641.
13. Zhang, H. and Liu, X., Analysis of milling energy in synthesis and formation mechanism of Mo disilicides by mechanical alloying. *Int. J. Refract. Met. Hard Mater.*, 2001, **19**, 203.
14. Magini, M. and Iasonna, A., Energy transfer in mechanical alloying (overview). *Mater. Trans. JIM*, 1995, **36**(2), 123.
15. Murty, B. S., Mohan Rao, M. and Ranganathan, S., Milling map and amorphization during mechanical alloying. *Acta Metall. Mater.*, 1995, **43**(6), 2443.
16. Burgio, N., Iasonna, A., Magini, M., Martelli, S. and Padella, F., Mechanical alloying of the Fe–Zr system: correlation between input energy and end products. *Nuovo cimento*, 1991, **13**, 459.
17. Lec, P.-Y., Chen, T.-R., Yang, J.-L. and Chin, T.-S., Synthesis of $MoSi_2$ powder by mechanical alloying. *Mater. Sci. Eng.*, 1995, **A192/193**, 556.
18. Ren, R., Yang, Z. and Shaw, L., A novel process for synthesizing nanostructured carbides: mechanically activated synthesis. *Ceram. Eng. Sci. Proc.*, 1995, **19**(4), 461.
19. Zeghmati, M., Duverger, E. and Gaffet, E., Mechanically activated self-propagating high temperature synthesis in the Fe–Al system. In *CANCAM 95—COMPTES RENDUS: Le 15è Congrès Canadien de Mécanique Appliquée*, ed. B. Tabarrok and S. Oost, 1995, pp. 952–953.
20. Yamada, K. and kamiya, N., High temperature mechanical properties of Si_3N_4–$MoSi_2$ and Si_3N_4–SiC composites with network structure of second phases. *Mater. Sci. Eng.*, 1999, **A261**, 270.
21. Hebsur, M. G., Choi, S. R., Whittenberger, J. D., Salem, J. A. and Noebe, R. D., Development of tough, strong, and pest-resistant $MoSi_2$-βSi_3N_4 composites for high-temperature structural applications. *NASA/TM*, 2001, 1.
22. Suryanarayana, C., Mechanical alloying and milling. *Prog. Mater. Sci.*, 2001, **46**(1–2), 1–184.
23. Rahouadj, R. and Gaffet, E., Shock transfer in ball milling: nanocomposite mechanical approach. *Gaffet - Mater. Sci. Forum*, 1996, **225–227**, 249.
24. Singh, S., Godkhindi, M. M., Krishnarao, R. V. and Murty, B. S., Synthesis of Si_3N_4–$MoSi_2$ in-situ composites from mechanically activated ($Mo + Si_3N_4$) powders. *J. Alloys Compd.*, 2004, **381**(1–2), 254–257.